

Thermal and Structural Analysis of Airborne Magnetic Data of Part of Nasarawa State, Nigeria: Implication for Geothermal Energy Exploration

Oladiran Johnson Abimbola¹ Taiwo Adewumi^{1*}, Hauwa Onyeka Iyima¹ & Fidelis Iorzua Kwaghhuwa²

¹Department of Physics, Federal University of Lafia, Nigeria

²Department of Geophysics, Federal University of Technology, Minna, Nigeria

Abstract

This study presents the results of thermal and structural analysis of airborne magnetic data of part of Nasarawa State, Nigeria. The study area is characterised by a complex geological setting, with numerous faults and fractures that may control geothermal activity. The Total Magnetic Intensity (TMI) of the study area was analysed using various techniques, including spectral analysis, Analytic signal (AS), Center for Exploration Targeting (CET), First vertical derivative (FVD), and second vertical derivative (SVD). The results of the CET, FVD, and SVD reveal a complex geological structural pattern, with numerous faults and fractures that may be related geothermal activity, trending mainly NE-SW direction. The AS map distinguished regions of high, intermediate, and low amplitude anomalies within the study area. The thermal analysis evaluated Curie point depth (CPD), geothermal gradient (GG), and heat flow (HF). Estimated values of CPD, GG, and HF range from 10 to 22.65 km, 25 to 55°C/km, and 60 to 140 mW/m², respectively. Feasible HF for geothermal resources were observed at the mid-portion of the northern region, corresponding to Mada, Nasarawa Egon, Akwanga, and at the western and south-eastern edges, covering Udeni and Keana. The delineated major structures in NE-SW direction might serve as migration conduits and channels for crustal HF within the study area. The results of this study have significant implications for geothermal exploration in the study area, and suggest that further investigation is warranted to determine the feasibility of geothermal energy production.

Keywords: Geothermal energy, heat flow, Curie point depth, renewable energy

Article History

Submitted

April 21, 2024

Revised

July 16, 2024

First Published Online

September 03, 2024

***Corresponding author**

T. Adewumi ✉

taiwo.adewumi@science.fulafia.edu.ng,

tydon4real@yahoo.co.uk

doi.org/10.62050/ljsir2024.v2n2.392

Introduction

The study area, located in north-central Nigeria, is an area of significant geological interest due to its complex tectonic history and potential for geothermal energy. Energy is a vital resource for national development. Nigeria, as a developing country, has over the years been retarded in advancement due to insufficient power generation and distribution. The current generating sources, which are hydropower stations and gas-powered stations, have their shortfalls. Hydro-stations have low output during dry seasons due to a shortage of water; gas stations emit greenhouse gases, which are not ecosystem-friendly and are discouraged globally. Imperatively, industrialization, which is a core component of economic development, is powered by an adequate supply of electricity. This places the country in dire need of filling a huge energy deficit, and geothermal energy, when harnessed, will offer the desired alternative [1, 2, 3, 4].

Geothermal energy is the heat produced in the internal layers of the earth, and studies have shown that two main sources contribute to the earth's internal heat, which are primordial heat and radiogenic heat. The Earth, though created more than 4.5 billion years ago, is continually cooling, thereby still retaining the blaze of

heat energy that birthed its formation and evolution in the form of primordial heat [5]. The radioactive decay of materials in the mantle and crust of the Earth produces daughter isotopes, releases geoneutrinos, and releases heat energy, also known as radiogenic heat. Three radioactive isotopes, uranium, thorium, and potassium, account for the majority of radiogenic heat due to their abundance in comparison to other radioactive isotopes [6, 7, 8].

Airborne magnetic data as a tool for studying the earth's subsurface relies on the magnetic susceptibility of rocks within the target regions. Over the years, studies have shown that aeromagnetic data is useful in identifying geologic structures such as faults, folds, shear zones, contacts, and intrusions, which are essential for localising magnetic minerals and delineating depth to geothermal reservoirs situated at the bottom of magnetic rocks [9, 10, 11, 12]. Numerous researches affirm the suitability of magnetic data for mapping geothermal anomalies both on a regional and concise scale [13, 14, 15, 16, 17, 18].

Suitable geophysical methods that could effectively and clearly image the subsurface and reveal the geothermal make up of study area is the pursuit of this study. Analysis of magnetic data will delineate geologic



structures (fractures, faults, shear zones) that could be associated with geothermal reservoirs; compute the Curie point depth, geothermal gradient, and heat flow from aeromagnetic data analysis. Inferences from the analyses will be used to map prospective areas for geothermal energy exploration.

Several studies attempting to estimate the geothermal framework of Nasarawa State and environs were done, employing various conventional geophysical and geological prospecting methods. Bore hole drilling, satellite imagery remote sensing, and airborne magnetic data analysis were applied at both regional and small-scale coverage [2, 15, 19, 20, 21, 22, 23].

It is the aim of this study to appropriately map the geothermal make up of study area via analysis of airborne magnetic data set. The estimation of heat flow trends and delineation of subsurface heat-conducting structural frameworks will further improve the reliability of the entire outcome of the study. The results of this study will provide useful geophysical information on geothermal potential within part of Nasarawa State. This could serve as a guide for potential investors in the energy sector who could leverage the generated data to harness the underlying potent resources.

Location and geologic settings of the study area

The study area is part of North Central Nigeria located precisely in Nasarawa State. It is bounded by Longitude 8.0° E to 9.0° E and Latitude 8.0° N to 9.0° N. The land cover is estimated to be 12, 100 km². The area cuts

across major towns such as Akwanga, Lafia, Wamba and Doma. An express way which links the Federal Capital Territory to Benue state capital Markudi passes across the study area from Northern part at Akwanga to southern part at Kardarko.

Geologically, the Middle Benue Trough (MBT) region is overlain by six Cretaceous formations including Asu River group, being the oldest, Ezeaku formation, Keana formation, Awe formation, Agwu formation and the Lafia formation which is the most recent in the stratigraphic succession [24, 25]. The Lafia formation which is also Maastrichtian, is part of the post-folding formation which terminated the sedimentation in the MBT. Within the study area, the sedimentary termination is seen as a demarcation along Nasarawa Eggon separating the sedimentary lithologies to the south and basement lithologies to the northern regions. The sediments are distinguished by sandstones, loose sands, flaky mudstones, alluvium, shale and limestones while the basement region is occupied by crystalline igneous intrusive such as porphyritic and biotite granite, migmatite, granite gneiss, undifferentiated schist and phylites, undifferentiated granite and migmatite [26]. The MBT was formed as a result of extensional tectonics during the break up of the super continent Gondwana in the Cretaceous stage. The trough was subjected to multiple phases of rifting, subsidence, and inversion, leading to formation of various structural features, including faults, folds, and fractures.

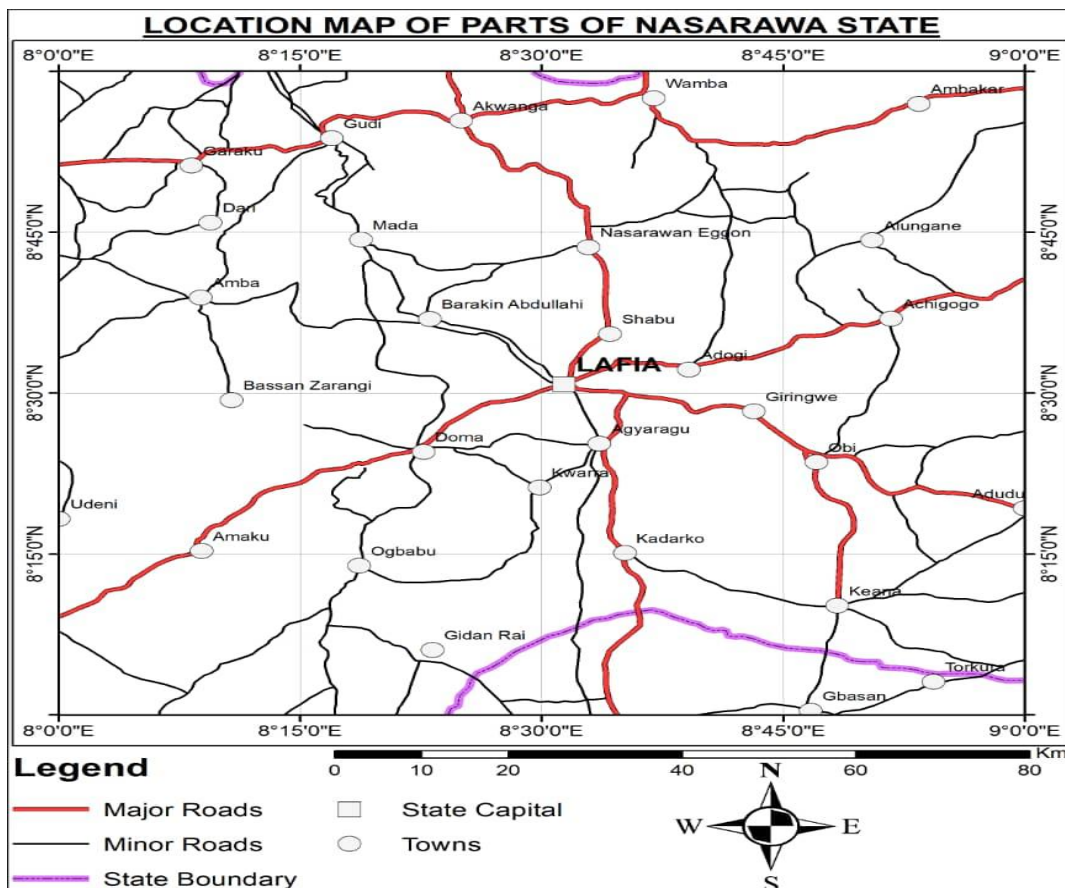


Figure 1: Location map of the study area (adapted from administrative map of Nigeria)

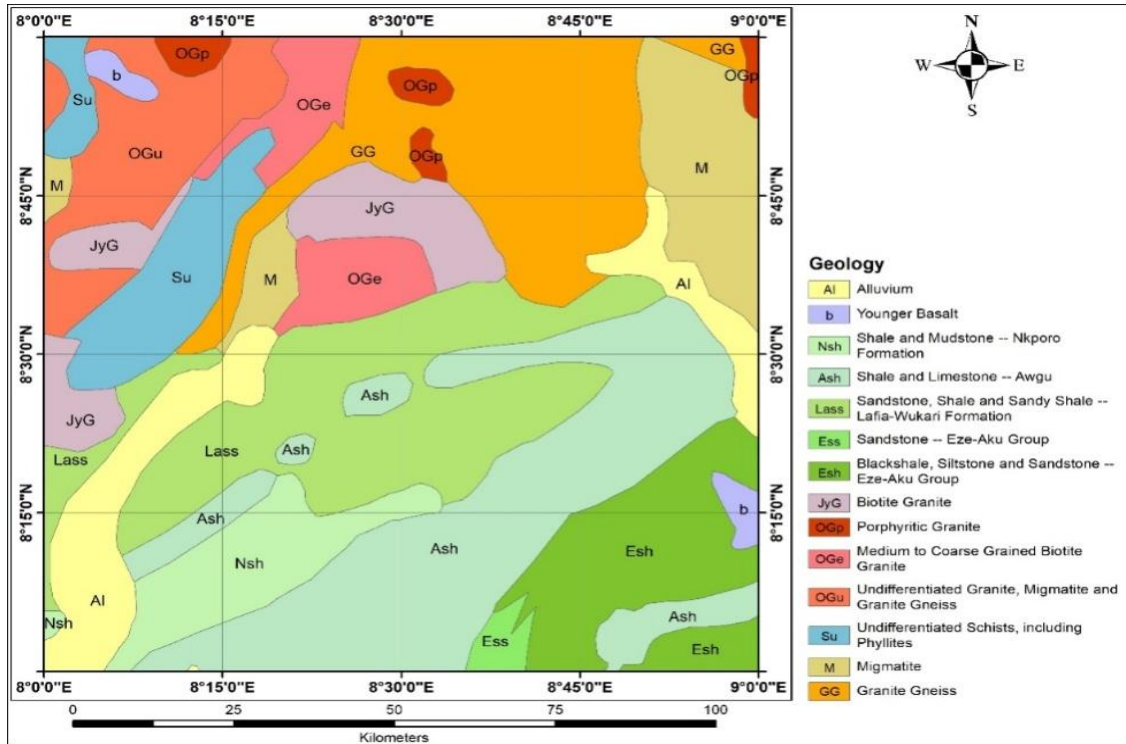


Figure 2: Geological map of the study area [27]

Materials and Methods

The airborne magnetic datasets used for this study were obtained from the Nigeria Geological Survey Agency (NGSA) [27]. A digital format of the high resolution airborne geophysical datasets was part of the nationwide data collected and pre-processed by Fugro Airborne Surveys. The pre-processing involved removal of offset, diurnal and International Geomagnetic Reference Field (IGRF) for the magnetic data while background radiation interactions were filtered from the radiometric data. The survey parameters and specifications for both data sets are presented in Table 1.

Table 1: Data parameter and specifications [27]

Survey Parameter	Magnetic Specifications	Radiometric Specifications
Data Acquired by:	Fugro Airborne Surveys	Fugro Airborne Surveys
Time Range	2005 – 2009	2005 – 2009
Data Recording Interval	0.1 seconds or less	0.1 seconds or less
Sensor Mean Terrain Clearance	80 meters	80 meters
Flight Line Spacing	500 meters	500 meters
Tie Line Spacing	5000 meters	2000 meters
Flight Line trend	135 degrees	135 degrees
Tie Line trend	45 degrees	45 degrees
Equipment: Aircraft	Cessna Caravan 208B ZS-FSA, Cessna Caravan 208 ZS-MSJ	Cessna Caravan 208B ZS-FSA, Cessna Caravan 208 ZS-MSJ
Equipment:	3 x Scintrex CS3 Cesium Vapour Magnetometer	(NaI “TI” crystals) 512-channels gamma-ray spectrometer

The area under investigation covers four (4) half-degree by half-degree (55 by 55 sq. km) data sheets of airborne magnetic and radiometric datasets which were knitted and used to produce the composite map of the total magnetic field (TMI) and the radioelement concentration maps (K, eTh, and eU) of the study area, respectively. All the datasets used for this study were filtered, enhanced, and processed using the Oasis Montaj™, Surfer, and MatLab software. The TMI gridded data were reduced to the magnetic equator to ensure proper placement of the magnetic anomalies over their causative bodies. Hence, the TMI reduced to equator (RTE-TMI) data were further analyzed to produce the vertical derivative (VD) maps, rose diagram (RD), analytic signal (ASG), and the geothermal parameter such as the CPD, geothermal gradient and heat flow. Also, the K, eTh, and eU were also utilised to generate the radiogenic heat production (RHP) maps. All the analysed maps were used to delineate the shallow-deep structural elements and thermal structures responsible for geothermal energy potential within the study area.

Geological structural mapping

Vertical derivative

The first vertical derivative is computed to help compress the deep sited magnetic source while enhancing the shallow and near surface features. For a study area located within the basement complex geology, the analysis will outline the geologic structural distortions, deformations and lineaments of magnetic sources. This will aid in amplifying the possibility of existing shallow Curie point depth underneath the near surface basement rock which is a pointer to potential



geothermal reservoir occurrence. The first vertical derivative is computed from the formula:

$$L(r) = r^n \quad (1)$$

where n depicts the order of differentiation generally 1 or 2, r signifies the wave-number in radians per ground unit and L is cycle/ground unit in which the survey was conducted e.g. metres, feet, kilometre.

Analytical signal

The analytical signal analysis estimates the amplitude response of magnetic anomalies. The method simplifies the location of causative bodies in magnetic data by generating a bell-shaped symmetrical function for two-dimensional bodies and amplifying it for three-dimensional bodies, independent of factors like strike, dip, and magnetization [28].

The analytic signal is a function related to magnetic fields by the derivatives:

$$AS = \sqrt{\left(\frac{\partial A}{\partial X}\right)^2 + \left(\frac{\partial A}{\partial Y}\right)^2 + \left(\frac{\partial A}{\partial Z}\right)^2} \quad (2)$$

Interpretation of analytic signal maps and images provides simple indications of magnetic source geometry, with half widths linearly related to depths if sources are vertical magnetic contacts [29].

Thermal structural mapping and heat flow Spectral depth analysis theory

The centroid method for evaluating depth to magnetic sources is reported as common and gives better depth estimates with few errors [30, 31]. The mathematical models of the centroid method are based on the examination of the shape of isolated magnetic anomalies introduced by Bhattacharyya and Leu [32] and the study of the statistical properties of magnetic ensembles by Spector and Grant [33]. Blakely [34] subsequently introduced power spectral density of total magnetic field, $\phi \Delta T(k_x, k_y)$ as:

$$\begin{aligned} \phi \Delta T(k_x, k_y) = \\ \phi_M(k_x, k_y) \cdot 4\pi^2 C_M^2 |\Theta_M|^2 |\Theta_f|^2 e^{-2|k|Z_t} (1 - \\ e^{-2k(Z_b - Z_t)})^2 \end{aligned} \quad (3)$$

where k_x and k_y are wave-numbers in x and y direction, $\phi_M(k_x, k_y)$ is the power spectra of the magnetization, C_M is a constant, Θ_M and Θ_f are factors for magnetization direction and geomagnetic field direction, and Z_b and Z_t are depths to bottom and top of magnetic layer, respectively.

If the layer's magnetization, $M(x, y)$ is a random function of x, y it implies that $\phi_M(k_x, k_y)$ is a constant, and therefore the azimuthally averaged power spectrum, $\phi(|k|)$ would be given as:

$$\phi(|k|) = A e^{-2|k|Z_t} (1 - e^{-2|k|(Z_b - Z_t)})^2 \quad (4)$$

The depth to the top of the magnetic source is therefore derived from the slope of the high-wave-number portion of the power spectrum as:

$$\ln \left(\frac{P}{P} \left(\frac{1}{k} \right) \right) = A - |k|Z_t \quad (5)$$

where $P(k)$ is the azimuthally averaged power spectrum, k is the wave-number ($2\pi \text{ km}^{-1}$), A is a

constant, and Z_t is the depth to the top of magnetic sources.

The centroid depth of magnetic sources can also be calculated from the low-wave-number portion of the wave-number-scaled power spectrum as [35]

$$\ln \left(\frac{P}{P} \left(\frac{1}{k} \right) \right) = B - |k|Z_0 \quad (6)$$

where B is a constant and Z_0 is the centroid depth of magnetic sources.

The depth to the bottom of the magnetic source (Z_b) can subsequently be obtained from the relation [30]

$$Z_b = 2Z_0 - Z_t \quad (7)$$

Using the depth to the bottom of magnetic sources (Z_b), the geothermal gradient $\left(\frac{dT}{dZ} \right)$ can be estimated as

$$\left(\frac{dT}{dZ} \right) = \left(\frac{\theta_c}{Z_b} \right), \quad (8)$$

where θ_c is the Curie temperature.

Next, using Z_b and $\frac{dT}{dZ}$, the heat flow (q_z) can similarly be estimated as [30]

$$q_z = -\sigma \left(\frac{\theta_c}{Z_b} \right) = -\sigma \left(\frac{dT}{dZ} \right), \quad (9)$$

where σ is thermal conductivity. Thermal conductivity of 2.5 W/m°C as the average for igneous rocks and a Curie temperature of 580°C are used as standard [36, 37].

Results and Discussion

Total magnetic intensity and reduce to equator maps

The trend of the magnetic signatures observed in the total magnetic intensity (TMI) and total magnetic intensity reduce-to-equator (TMI-RTE) maps recorded in nano tesla are represented in aggregate of colours over the study area (Fig. 3a and b). The spatially distributed values range from -41.4 to 113.8 nT and -35.9 to 111.2 nT, respectively. The TMI was reduced to magnetic equator using geomagnetic inclination and declination values of -7.33° and 1.62° respectively. The RTE filter enhances the position of magnetic anomalies above their magnetic sources or causative bodies. The northern regions are generally covered by high intensity values depicted in red to pink colours, which might be attributable to the dominant crystalline rocks. These include areas such as Akwanga, Mada, and Garaku in the northwestern regions, and Wamba, Nassrawa-Egon and Amboke on the northeastern regions. A sharp contrast of magnetic signatures is seen in the central and southwestern regions, corresponding to the Lafia and Udeni areas, respectively. These regions are depicted in deep blue colours signifying low magnetic intensities. The larger parts of southeastern regions with parts of south west are covered in yellow-red and green colours respectively signifying medium intensity values. The southern regions generally are covered by sedimentary rock formations that are low in magnetic susceptibility. Comparing the TMI-RTE to TMI, the RTE map (Fig. 3b) of the study area reveals more aligned magnetic signatures over their causative bodies.

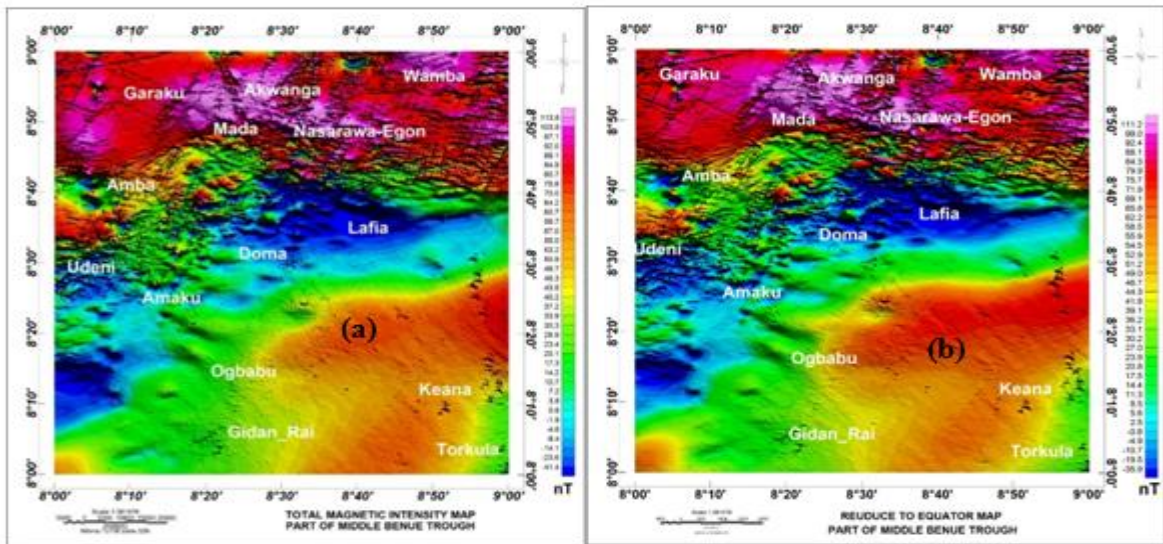


Figure 3: (a) Total magnetic intensity map and (b) TMI reduce to magnetic equator map of the study area

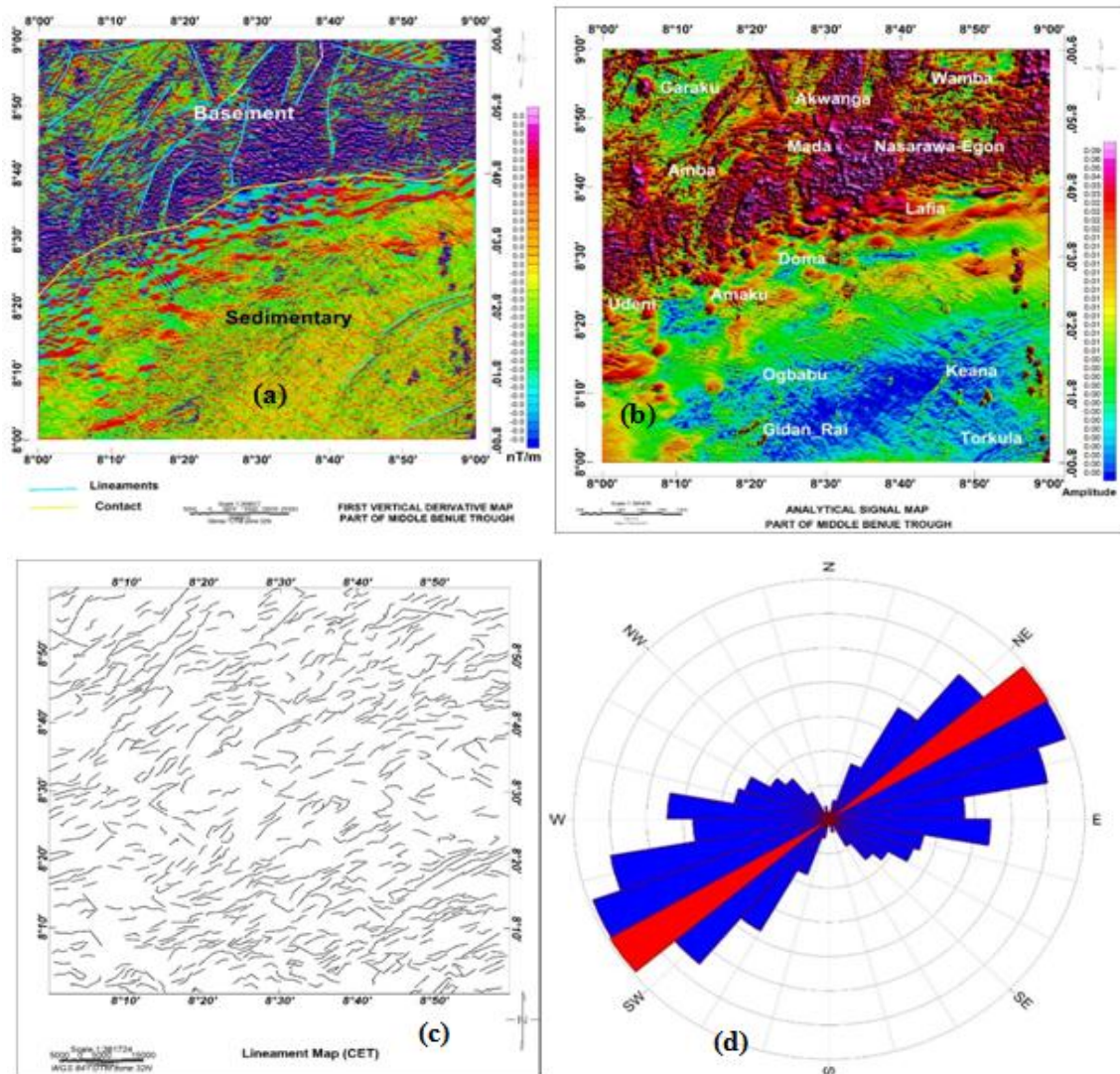


Figure 4: (a) Vertical derivative map (b) Analytical signal map (c) Lineament map and (d) Rose diagram map the of study area



Delineation of structural trends

The first vertical derivative (FVD) map (Fig. 4a) is a measure of short- and long-wavelength anomaly trends. The short-wavelength anomalies at high frequencies are observed as distorted magnetic signatures occurring mainly in the northern half of the study area. They also signify shallow depth for magnetic sources, which are typical of basement terrains. The long-wavelength anomalies are observed in the southern half of the study area; they denote low magnetic intensities, which can be associated with sedimentary terrains. The blue lines on the first vertical derivative are the magnetic lineaments, while the yellow line indicates a lithological contact profile cutting across the study area in the middle region. The contact shows the termination of basement and sedimentary formations in the study area. The delineated lineaments in NE-SW, NW-SE direction on the first vertical derivative map can be associated with geologic structures such as fractures, folds, fault lines, and shear zones.

The analytical signal (AS) (Fig. 4b) is one of the analyses for delineating and enhancing geologic structures within the area of study. It is a measure of amplitudes computed to represent outcrops and shallow and deep-sited magnetic sources. The result clearly separates the northern regions of the study area, which are clustered by geologic structures, from the southern regions, which are devoid of near-surface structures. The northern regions mapped in red to pink colors can be associated with outcrops or shallow-sited magnetic sources with an amplitude range of 0.02 to 0.09. The near-surface features also signify basement complex terrane, while the low amplitudes ranging from 0.00 to 0.01 are regions of thick sedimentation and deeply sited magnetic sources. The regions of low amplitudes are observed from the middle regions towards the south and are more prominent at the south-eastern edge of the study area.

The lineaments map (Fig. 4c) shows the alignment of linear magnetic signatures, which can be associated with the geologic structural framework of the study area. Densely clustered lineaments are observed at the northern regions and the south-eastern edge. Both major and minor lineaments reflect structural deformations in basement rocks in the northern half and sedimentary formations in the southern regions of the study area. Geologic structures such as fractures, fault lines, folds, contacts, dykes, and shear zones are the results of various degrees of crustal deformation. Major lineaments are linked with elongated structures, while minor lineaments denote short distortions.

The rose diagram (RD) (Fig. 4d) is a representation of the directional trend of how structures are aligned within the study area. Major and minor structures are trending in the NE-SW, NNE-SSW, and E-W direction. The major structures delineated in Fig. 4a and 4b might serve as passage for the crustal heat, which might be utilised for geothermal energy in the study area.

Estimating the Curie point depth, geothermal gradient, and heat flow

For this study, sixteen (16) overlapping sub-sheets were mapped out and each subjected to Fast Fourier Transform (FFT) analysis. This process decomposes the magnetic data into its wave and energy spectral components. Both components were plotted using MATLAB with the log of energy on the vertical axis and the wave-number component on the horizontal axis (Fig. 5). A straight line is fitted at the lower and higher wave-number portions of the graph to generate gradients corresponding to the depth to the centroid (Z_0) and depth to the top (Z_t) of magnetic sources, respectively. The CPD is calculated from the values of depth to the centroid and top of magnetic sources using equation (7). The geothermal gradient is obtained when the Curie point depth is inputted into equation (8). Both CPD and geothermal gradient were used as inputs in equation (9) to evaluate the heat flow using a thermal coefficient of 2.5.

The geothermal parameters were obtained for each of the sixteen sub-sheets, and a coordinate corresponding to the centre of each sub-sheet was recorded (Table 1). Recorded coordinates for sixteen sub-sheets and values for each parameter were inputted into contouring software (Surfer Version 20). The resultant contour maps for Curie point depth, geothermal gradient, and heat flow were generated to show the prevailing trend of each parameter across the study area.

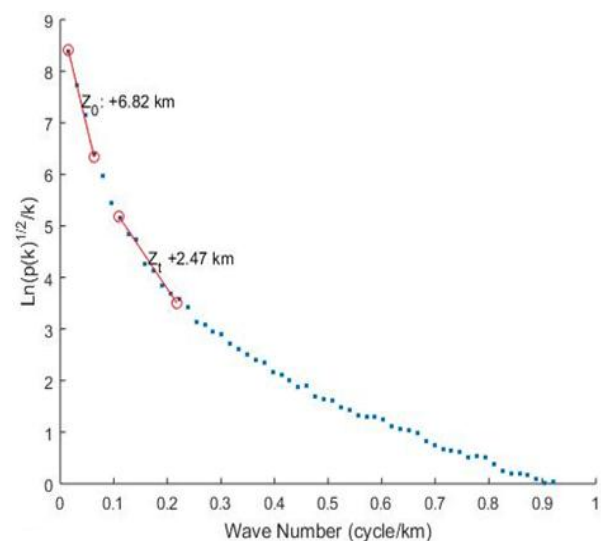


Figure 5: Spectral plot for block 1 indicating depth to top (Z_t) and centroid (Z_0)

The CPD map of the study area (Fig. 6a) is a reflection of the depths to the bottom of magnetic sources mapped across the study area. The depth ranges indicate how far from the earth surface the Curie temperature of 580°C can be reached. Estimated values ranged from 10 to 23 km, with an average of 16.30 km. The regions just above the central area, extending to the north-eastern regions, recorded deeper depths of 18 to 23 km.

The deeper depths are mapped within the regions corresponding to Lafia, Shabu, and Aungane, depicted in blue to sky blue colors on the map. The north-west to south-western regions are mapped with a shallow depth range of 10 to 15 km. Areas such as Garaku, Amba, Bassan Zarangi, Udeni, Amaku, and part of Doma are mapped within the regions depicted in yellow, red, and purple colors on the map with a depth below 15 km. The geothermal gradient (Fig. 6b) shows the variation of temperature with depth in kilometers; it's also a characteristic of the temperature gradients across the various regions of the study area. High values can be associated with potential geothermal reservoirs, while low values could denote a normal or no geothermal prospect. Within the study area, high temperature gradients are recorded along the northwest down to the southwestern regions. Estimated values ranging from 25 to 55°C/km were recorded, with an average of 37.40°C/km. The high ranges of 43 to 55°C/km are

depicted in yellow to orange colors. North-eastern areas such as Mada, Barakin Abdullahi, Adogi, Shabu, Lafia, and Achigogo are depicted in blue to purple, indicative of a low temperature gradient. The heat flow map (Fig. 6c) reflects the geothermal makeup of the study area. Estimated values of 60 to 140 mW/m² were recorded, with an average of 93.88 mW/m². A range of heat flow above 80 mW/m² is considered high and meets an exploitable threshold. The entire study area shows prevailing heat flow values above 80 mW/m², with the exception of areas around Wamba in the central to north-eastern region. The northwest, down to the southwestern regions, recorded peak values from 110 to 140 mW/m² within areas such as Garaku, Dari, Amba, Bassan Zarangi, Udeni, Amaku, Ogbabu, and Gidanrai. The south-eastern regions recorded values between 85 and 110 mW/m².

Table 1: Evaluated CPD, geothermal gradient, and heat flow of study area

BLK	Lon	Lat	Depth to Centroid Z ₀ (km)	Depth to Top Z _t (km)	Depth to Bottom Z _b (km)	Geothermal Gradient (°C/km)	Heat Flow (mW/m ²)
1	8.25	8.75	6.82	2.47	11.17	51.92	130.32
2	8.42	8.75	10.5	2.23	18.77	30.90	77.56
3	8.58	8.75	8.34	3.34	13.34	43.48	109.13
4	8.75	8.75	10.5	1.56	19.45	29.82	74.85
5	8.25	8.58	6.51	1.42	11.60	50.00	125.5
6	8.42	8.58	12.5	3.20	21.80	26.61	66.79
7	8.58	8.58	12.0	3.40	20.60	28.16	70.68
8	8.75	8.58	12.0	1.35	22.65	25.61	64.28
9	8.25	8.42	10.3	4.36	16.24	35.71	89.63
10	8.42	8.42	8.06	2.23	13.89	41.76	104.8
11	8.58	8.42	9.90	2.76	17.04	34.03	85.44
12	8.75	8.42	9.83	2.78	16.88	34.36	86.24
13	8.25	8.25	7.04	3.41	10.67	54.36	136.44
14	8.42	8.25	8.80	2.77	14.83	39.11	98.17
15	8.58	8.25	9.61	3.08	16.14	35.94	90.21
16	8.75	8.25	9.92	4.04	15.80	36.71	92.14

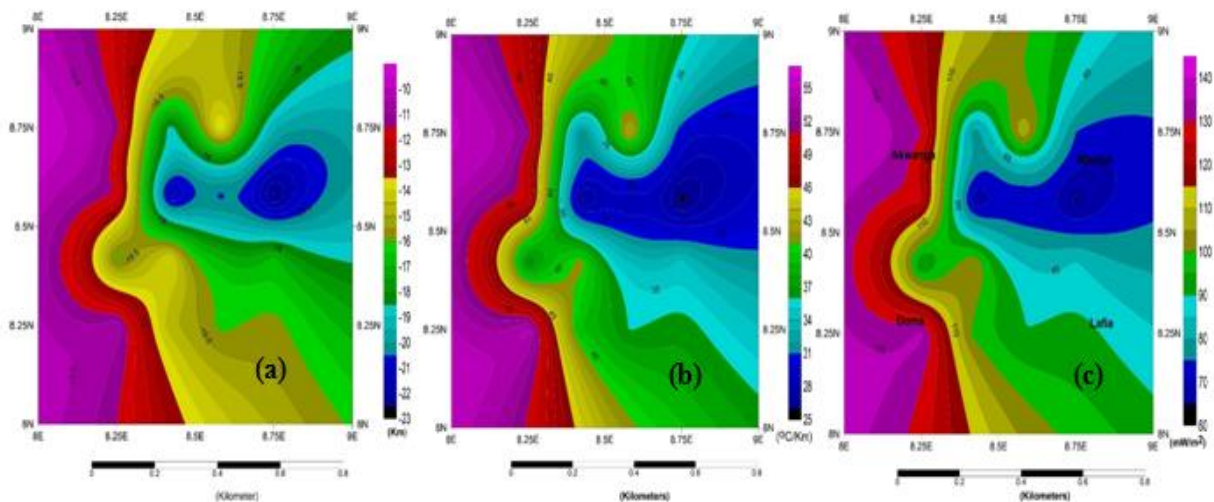


Figure 6: Contour map of; (a) CPD (b) geothermal gradient and (c) heat flow of the study area



The study area is comprised of two major lithological units; crystalline basement complex and sedimentary rocks. The basement complex occupies the northern portion of the study area and made up of Granite Gneiss, Migmatite, medium to coarse Biotite Granite, undifferentiated Granite, Biotite Granite, undifferentiated Schist, and porphyritic granite. On the other hand, the southern part of the study area is dominated by sedimentary rocks, which are made up of Alluvium, shale and mudstone, shale, limestone, and sandstone (Fig. 2). The high magnetic signatures observed in the northern part might be attributable to the dominated crystalline rocks. The low magnetic anomalies in the southern part might result from the dominated sedimentary rocks with little or no magnetic susceptibility.

Geological structures such as faults and lineaments play a significant role in geothermal prospecting. They serve as a vent/conduit for the migration of heat generated and stored in the geothermal reservoir to its manifestation on the earth's surface. The structural trends within the study area were effectively delineated using FVD, AS, RD, and lineament map generated from centre for exploration targeting (CET) (Fig. 4a-d). Both minor and major structures were delineated with major structures oriented in NE-SW, NNE-SSW, and NW-SE directions. The dominant structural trending can be inferred from the RD and lineament maps (Fig. 4c-d). These structures can be associated with geologic structures such as faults, fractures, folds, and shear zones. The occurrence of these structures can be linked with possible vents and conduit channels through which geothermal energies reaches the earth surface from the geothermal reservoir.

Viable areas within the study for geothermal resources

The results of the spectral analysis indicate high geothermal parameters in all regions, with the exception of areas around Lafia extending to the eastern edge of the study area. This implies that all other regions recorded values of 80 mW/m² and above, which is favourable for good geothermal sources [38, 39]. These range of result values also aligns with outcomes of previous regional researches involving Akinyemi and Zui [40], Abdullahi *et al.* [41], Dopamu *et al.* [20] and Salako *et al.* [2]. The trend of estimated heat flow also compares favourably with results obtained via satellite imagery and regional gravity data analysis within the Middle Benue Trough [19].

The regions of interest for mapping geothermal zones will be areas with positive geothermal parameters from spectral analysis of magnetic data. It can be deduced that regions of high heat flow within 85 to 110 mW/m² might be attributable to geological stability, similar lithology, thermal conductivity, and geothermal gradient of the study area. These ranges of values from the analyses meet recommended estimates for a viable geothermal source. Hence, the areas of Mada, Nasarawa-Egon and Akwanga at the mid portion of northern region, Udeni at western edge with Ogbabu, Keana and Torkula at south eastern region, are areas

noted to have features that favour geothermal exploration within the study area.

Conclusion

The comprehensive analysis of airborne magnetic data within part of the middle Benue trough revealed a clearer image of subsurface geothermal compositions within the study area. The results of the spectral depth analysis performed on the airborne magnetic data evaluated the essential parameters that were indicative of a good geothermal prospect. Geologic features, including fault lines, shear zones, folds, and fractures, can be linked to the defined lineaments on the first vertical derivative map. The presence of these formations in the study area may be connected to potential vents and conduit channels that allow geothermal energy to reach the earth's surface. Sufficient research shows that shallow Curie point depth, a high geothermal gradient, and heat flow favor the siting of a good geothermal source. Shallow CPD and anomalous heat flow of 110 to 140 mW/m² were recorded in the western regions (NW and SW), indicating a highly resourceful geothermal region. Other regions of the study area, with the exception of the central regions extending to the eastern edge, recorded heat flow values of 85 to 110 mW/m². These ranges of values fall within the conventional threshold of a good geothermal source and denote a wide coverage of ripped geothermal zones across the study area.

The delineated geological structures and geothermal parameters collaboratively map zones of prospective viable geothermal sources. Regions of high heat flow coinciding subsurface pathways are mapped as geothermal prospective zones. These areas are: Mada, Nasarawa-Egon, and Akwanga in the mid-northern regions; Udeni at the western edge; and Ogbabu, Keana, and Torkula in the south-eastern region.

A direct geophysical method such as the magnetotelluric method can further be used in the delineated geothermal anomalous zones for geothermal resource exploitation in the study area. The harnessed geothermal energy will be used to complement the existing energy base of the study area and its environs.

Conflict of interests: The authors declare that they have no conflict of interests.

Acknowledgement: This research was supported by a 2024 Institutional Based Research (IBR) grant from the Tertiary Education Trust Fund (TETFund) of Nigeria. Hence, the authors wish to appreciate TETFund for the funding of this research.

References

- [1] Eletta, B. E., & Udensi, E. E. (2012). Investigation of the Curie point isotherm from the magnetic fields of eastern sector of central Nigeria. *Geosciences*, 2(4), 101-106.
- [2] Salako, K. A., Adetona, A. A., Rafiu, A. A., Alahassan, U. D., Aliyu, A. & Adewumi, T., (2020). Assessment of geothermal potential of parts of Middle Benue Trough, North-East Nigeria. *J. of the Earth and Space Phy.*, 45(4), <https://doi.org/10.22059/jesphys.2019.260257.1007017>
- [3] Adewumi, T., Salako, K. A., Usman, A. D., & Udensi, E. E. (2021). Heat flow analyses over Borno Basin and its environs, Northeast Nigeria, using airborne magnetic and radiometric data: implication for geothermal energy prospecting. *Arabian Journal of Geosciences*, 14, 1-19.
- [4] Adetona, A. A., Fidelis, I. K. & Shakarit, B. A. (2023). Interpreting the magnetic signatures and radiometric indicators within Kogi State, Nigeria for economic resources. *Geosystems and Geoenvironment*, 2(2), 100157.
- [5] Lay, T., Hernlund, J. & Buffett, B. A. (2008). Core–mantle boundary heat flow. *Nature Geoscience*, 1(1), 25-32.
- [6] Schmeling, H., Marquart, G., Weinberg, R., & Wallner, H. (2019). Modelling melting and melt segregation by two-phase flow: new insights into the dynamics of magmatic systems in the continental crust. *Geophysical Journal International*, 217(1), 422-450.
- [7] Kuforijimi, O. & Christopher, A. (2017). Correlation and mapping of geothermal and radioactive heat production from the Anambra Basin, Nigeria. *African J. of Environmental Science and Techn.* 11(10), 517-531. <https://doi.org/10.5897/AJEST2017.2382>
- [8] Korenaga, J. (2011). Clairvoyant geoneutrinos. *Nature Geoscience*, 4(9), 581-582.
- [9] Ravat, D., Pignatelli, A., Nicolosi, I. & Chiappini, M., (2007). A study of spectral methods of estimating the depth to the bottom of magnetic sources from near-surface magnetic anomaly data. *Geophysical Journal Int.* 169, 421–434. <https://doi.org/10.1111/j.1365-246X.2007.03305.x>
- [10] Paterson, N. R. & Reeves, C. V. (1985). Applications of gravity and magnetic surveys: the state-of-the-art in 1985. *Geophy.*, 50(12), 2558-2594. <https://doi.org/10.1190/1.1441884>
- [11] Airo, M. (2002). Aeromagnetic and aeroradiometric response to hydrothermal alteration. *Surveys in Geophysics*, 23, 273-302. <https://doi.org/10.1023/A:1015556614694>
- [12] Adewumi, T., Salako, K.A., Adediran, O.S., Okwoko, O.I., Sanusi Y.A. (2019). Curie point depth and heat flow analyses over part of Bida Basin, North Central Nigeria using Aeromagnetic Data. *Journal of Earth Energy Engineering*, 8(1).
- [13] Abdelrahman, K., Ekwok, S. E., Ulem, C. A., Eldosouky, A. M., Al-Otaibi, N., Hazaea, B. Y., ... & Akpan, A. E. (2023). Exploratory mapping of the geothermal anomalies in the Neoproterozoic Arabian Shield, Saudi Arabia, using magnetic data. *Minerals*, 13(5), 694.
- [14] Melouah, O., Ebong, E. D., Abdelrahman, K. & Eldosouky, A. M. (2023). Lithospheric structural dynamics and geothermal modeling of the Western Arabian Shield. *Scientific Reports*, 13(1), 11764.
- [15] Alfaifi, H. J., Ekwok, S. E., Ulem, C. A., Eldosouky, A. M., Qaysi, S., Andr  s, P. & Akpan, A. E. (2023). Exploratory assessment of geothermal resources in some parts of the Middle Benue Trough of Nigeria using airborne potential field data. *Journal of King Saud University-Science*, 35(2), 102521.
- [16]   erm  k, V. & Rybach, L. (1982). Thermal conductivity and specific heat of minerals and rocks. *Landolt-B  rnstein: Numerical Data and Functional Relationships in Sci. and Techn., New Series, Group V (Geophy. and Space Research), Volume Ia (Physical Properties of Rocks)*, edited by G. Angenheister, Springer, Berlin-Heidelberg, 305-343.
- [17] Ekwok, S. E., Akpan, A. E., Ebong, E. D. & Eze, O. E. (2021). Assessment of depth to magnetic sources using high resolution aeromagnetic data of some parts of the Lower Benue Trough and adjoining areas, Southeast Nigeria. *Advances in Space Res.*, 67(7), 2104-2119.
- [18] Adetona, A. A., Rafiu, A. A., Aliyu, B. S., John, M. K. & Kwaghua, I. F. (2024). Estimating the heat flow, geothermal gradient and radiogenic heat within the young granites of Jos Plateau North Central Nigeria. *Journal of the Earth and Space Physics*, 49(4). https://jesphys.ut.ac.ir/article_95497.html
- [19] Ngene, T., Mukhopadhyay, M. & Ampana, S. (2022). Reconnaissance investigation of geothermal resources in parts of the Middle Benue Trough, Nigeria using remote sensing and geophysical methods. *Energy Geoscience*, 3(4), 360-371.
- [20] Dopamu, K. O., Akoshile, C. O. & Nwankwo, L. I. (2021). Regional estimation of geothermal resources of the entire Benue Trough, Nigeria using high-resolution aeromagnetic data. *Geomechanics and Geophysics for Geo-Energy and Geo-Resources*, 7, 1-17.
- [21] Abdullahi, M. & Kumar, R. (2020). Curie depth estimated from high-resolution aeromagnetic data of parts of lower and middle Benue trough (Nigeria). *Acta Geodaetica et Geophysica*, 55(4), 627-643.
- [22] Anudu, G. K., Onuba, L. N., Onwuemesi, A. G. & Ikpokonte, A. E. (2012). Analysis of aeromagnetic data over Wamba and its adjoining areas in north-central Nigeria. *Earth Sciences Research Journal*, 16(1), 25-33.



- [23] Bako A. S. J. (2010). Geothermal energy potential in the part of middle Benue trough located in Nasarawa state. *A thesis submitted to the Postgraduate School, Ahmadu Bello University, Zaria, Nigeria.*
- [24] Offodile, M. E. (1976). The geology of the Middle Benue, Nigeria. *Palaentological Institute, Uppsala University, Special Publication*, 4, 1–166.
- [25] Nwajide, C. S. (1990). Cretaceous sedimentation and paleogeography of the central Benue Trough. *The Benue. Tough structure and Evolution International Monograph Series, Braunschweig*, 19-38.
- [26] Obaje, N. G. (2009). *Geology and Mineral Resources of Nigeria* (Vol. 120, p. 221). Berlin: Springer.
- [27] Nigeria Geological Survey Agency, 2009. Geological Map of Nigeria <https://ngsa.gov.ng/geological-maps>
- [28] Debeglia, N., & Corpel, J. (1997). Automatic 3-D interpretation of potential field data using analytic signal derivatives. *Geophysics*, 62(1), 87-96
- [29] Roest, W. R., Verhoef, J. & Pilkington, M. (1992). Magnetic interpretation using the 3-D analytic signal. *Geophysics*, 57(1), 116-125.
- [30] Okubo, Y., Graf, R. J., Hansen, R. O., Ogawa, K., & Tsu, H. (1985). Curie point depths of the island of Kyushu and surrounding areas, Japan. *Geophysics*, 50(3), 481-494.
- [31] Bhattacharyya, B. K. & Leu, L. K. (1977). Spectral analysis of gravity and magnetic anomalies due to rectangular prismatic bodies. *Geophysics*, 42(1), 41-50.
- [32] Bhattacharyya, B. K. & Leu, L. K. (1975). Spectral analysis of gravity and magnetic anomalies due to two-dimensional structures. *Geophysics*, 40(6), 993-1013.
- [33] Spector, A. & Grant, F. S. (1970). Statistical models for interpreting aeromagnetic data. *Geophysics*, 35(2), 293-302.
- [34] Blakely, R. J. (1996). *Potential Theory in Gravity and Magnetic Applications*. Cambridge University Press.
- [35] Tanaka, A., Okubo, Y. & Matsubayashi, O. (1999). Curie point depth based on spectrum analysis of the magnetic anomaly data in East and Southeast Asia. *Tectonophysics*, 306(3-4), 461-470.
- [36] Stacey, F. D. (1977). A thermal model of the earth. *Physics of the Earth and Planetary Interiors*, 15(4), 341-348.
- [37] Trifonova, P., Zhelev, Z., Petrova, T. & Bojadgieva, K. (2009). Curie point depths of Bulgarian territory inferred from geomagnetic observations and its correlation with regional thermal structure and seismicity. *Tectonophysics*, 473(3-4), 362-374.
- [38] Cull, J.P. & Conley, D., (1983). Geothermal gradients and heat flow in Australian sedimentary basin. *J. Aust. Geol. Geophys.*, 8, 32–337.
- [39] Jessop A. M. (1976). Geothermal energy from sedimentary basins. *United State Department of Energy Office of Scientific and Technical Information*. NP. 22308. EDB-77-131177
- [40] Akinyemi, L. & Zui, V. I. (2019). Summary of heat flow studies in Nigeria. *J. Belarusian State Univ. Geogr. Geol.*, 2, 121–132. <https://doi.org/10.33581/2521-6740-2019-2-121-132>
- [41] Abdullahi, M., Valdon, Y. B., Andrew, F. P. & Idi, B. Y. (2023). Curie depth and surface heat flow estimation from anomalous magnetic blocks in the lower and part of Middle Benue Trough and Anambra Basin. *Earth and Planetary Science*, 2(1), 11-20.

Citing this Article

Abimbola, O. J., Adewumi, T., Iyima, H. O. & Kwaghua, F. I. (2024). Thermal and structural analysis of airborne magnetic data of part of Nasarawa State, Nigeria: Implication for geothermal energy exploration. *Lafia Journal of Scientific and Industrial Research*, 2(2), 145 – 154. <https://doi.org/10.62050/ljsir2024.v2n2.392>